Supporting Information

for

Electronic Structure and Carrier Mobility of Two-dimensional α Arsenic Phosphide

Fazel Shojaei

Department of Chemistry and Bioactive Material Sciences and Research Institute of Physics and Chemistry, Jeonbuk National University, Jeonju, Chonbuk 561-756, Republic of Korea

and

Hong Seok Kang*

Department of Nano and Advanced Materials, College of Engineering, Jeonju University, Hyoja-dong, Wansan-ku, Chonju, Chonbuk 560-759, Republic of Korea

*Corresponding author: hsk@jj.ac.kr

A full list of Ref. 15 is given below:

Liu, B.; Kopf, M.; Abbas, A. N.; Wang, X.; Guo, Q.; Jia, Y.; Xia, F.; Weihrich, R.; Bachhuber, F.; Pielnhofer, F.; Wang, H.; Shall, R.; Cronin, S. B.; Ge, M.; Fang, X.; Nilges, T. Black Arsenic–Phosphorus: Layered Anisotropic Infrared Semiconductors with Highly Tunable Compositions and Properties. *Adv. Mater.* **2015**, DOI: 10.1002/adma.201501758.

Methods for calculating of effective mass, elasticity modulus, and deformation potential:

1. Effective mass:

   For example, we include 6~7 *k*-points around the valence band maximum within 0.1 eV to perform a parabolic fit, which corresponds to R^2 value of 0.99. Table 2 shows that the effective mass thus calculated is quite close to those presented in Ref. 2 for α phosphorene.

2. Elastic modulus:

   The elastic modulus C_{2D} of the longitudinal strain in the propagation directions (both x and y) of the longitudinal acoustic wave is derived from $(E - E_0)/S_0 = C(\ell/\ell_0)^2/2$, where E is the total energy and S_0 is the lattice surface at equilibrium for a 2D system. In our calculation, five different strains, i.e., [-1%, -0.5%, 0, 0.5%, 1%] were taken into the fitting, along each of X and Y directions.

3. Deformation potential:

   In a way similar to the case of fitting for the elastic modulus, we sample a series of five steps of dilation with 0.5% interval for the curve fitting of ΔE_i. For more details, readers can refer to Figure 5 in Supplementary Information of Ref. 2. Also note that our calculated values for α phosphorene are in reasonable agreements with those from Ref. 2. We recall that Ref. 2 uses optB88-mJB for structure optimization, not the PBE-D3 adopted in our work. That difference should be responsible for the small difference in the deformation energy obtained in our work from that shown in Ref. 2.

Figure S1 Charge density distributions of the VB (a) and CB (b) at the Γ -point for the α_1 AsP.

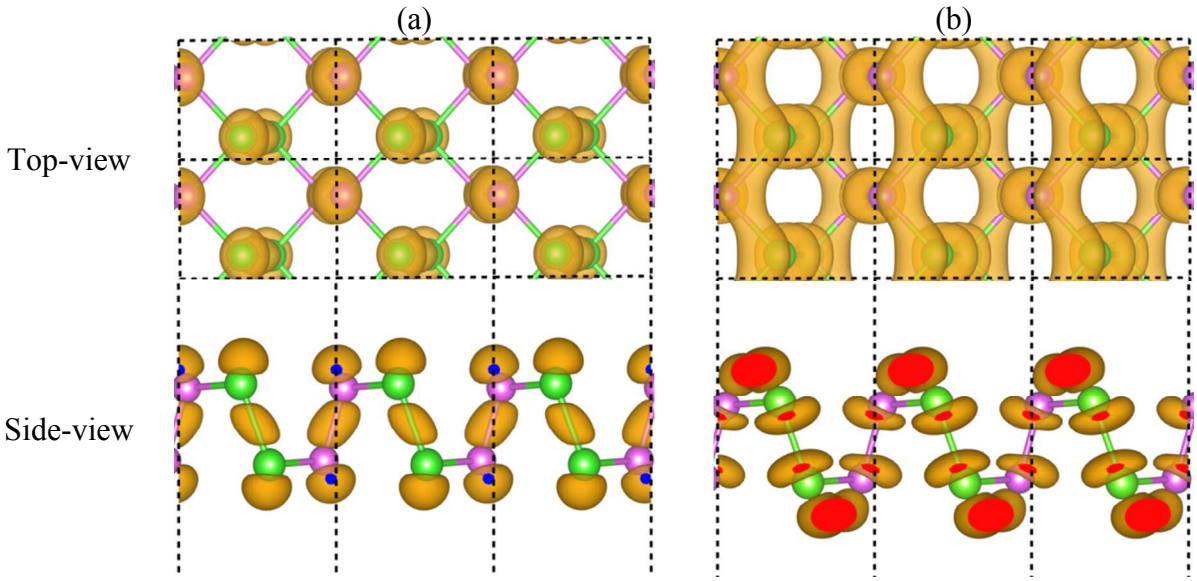

Figure S2 Charge density distributions of the VB (a, c) and the CB (b, d) for the α_1 AsP at the X' and Y points, respectively. Noted that those for the α_2 AsP and the α_3 AsP at those points exhibit similar characteristics.

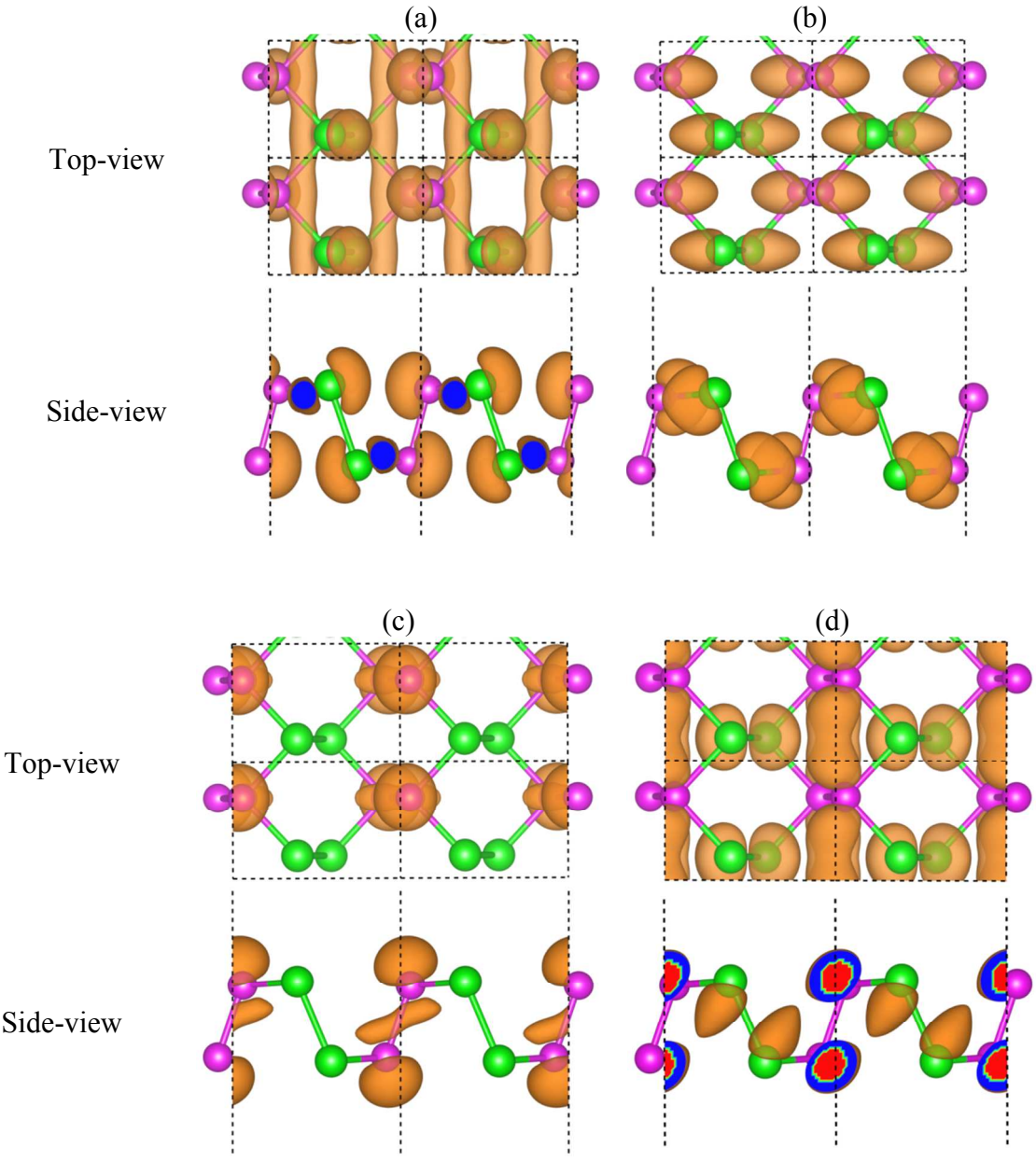

Figure S3 Strain energy per atom in unit of eV versus isotropic biaxial ($\sigma_{ac}:\sigma_{zz}=1:1$) or uniaxial strain ($\sigma_{zz}$ or σ_{ac}) along the armchair or zigzag direction, respectively, (a) and anisotropic biaxial strain ($\sigma_{ac}:\sigma_{zz}=3:1$ or $\sigma_{ac}:\sigma_{zz}=4:1$) (b) for the α_1 and the α_3 AsP in comparison with those for α P.

(a)

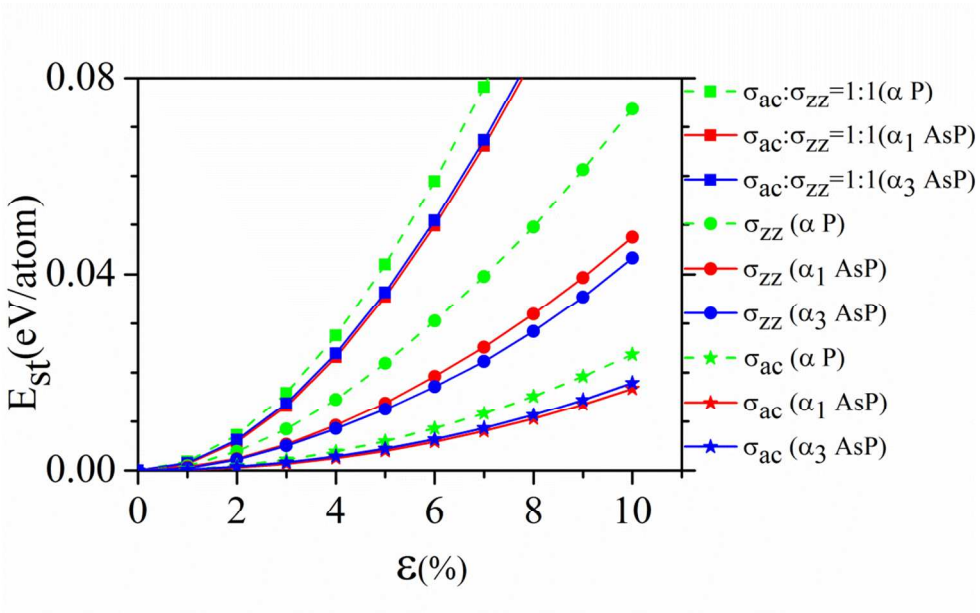

(b)

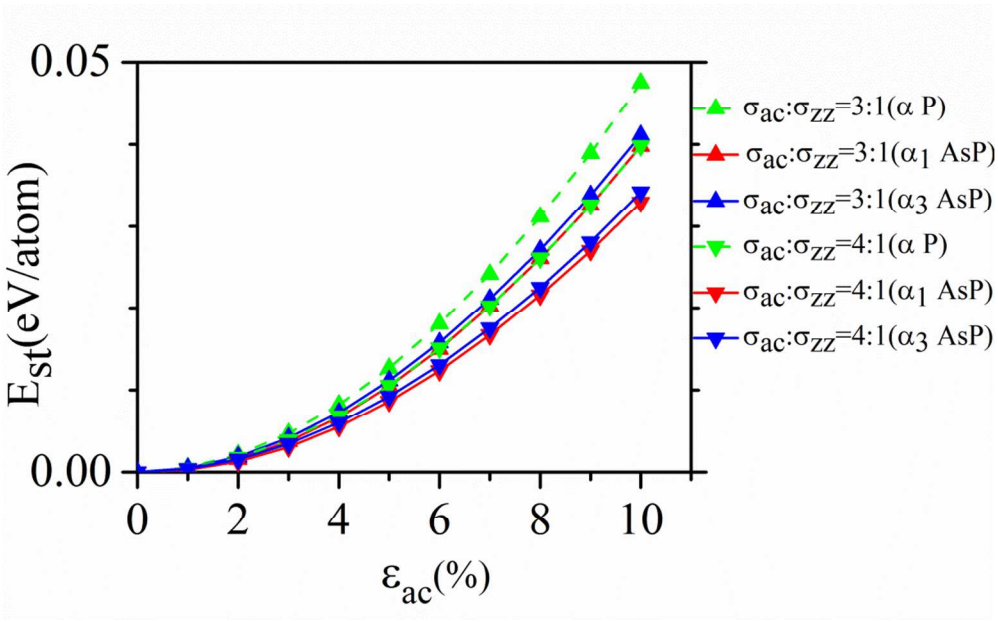
0.05
0.00
E_{st}(eV/atom)
0
2
4
6
8
10
ε_{ac}(%)
σ_{ac}:σ_{ZZ}=3:1(α P)
σ_{ac}:σ_{ZZ}=3:1(α_1 AsP)
σ_{ac}:σ_{ZZ}=3:1(α_3 AsP)
σ_{ac}:σ_{ZZ}=4:1(α P)
σ_{ac}:σ_{ZZ}=4:1(α_1 AsP)
σ_{ac}:σ_{ZZ}=4:1(α_3 AsP)

Figure S4 Change of the lattice constant along the direction normal tot the applied uniaxial strain (σ_{zz} or σ_{ac}) for the α_1 (a) and the α_3 (b) AsP.

(a)

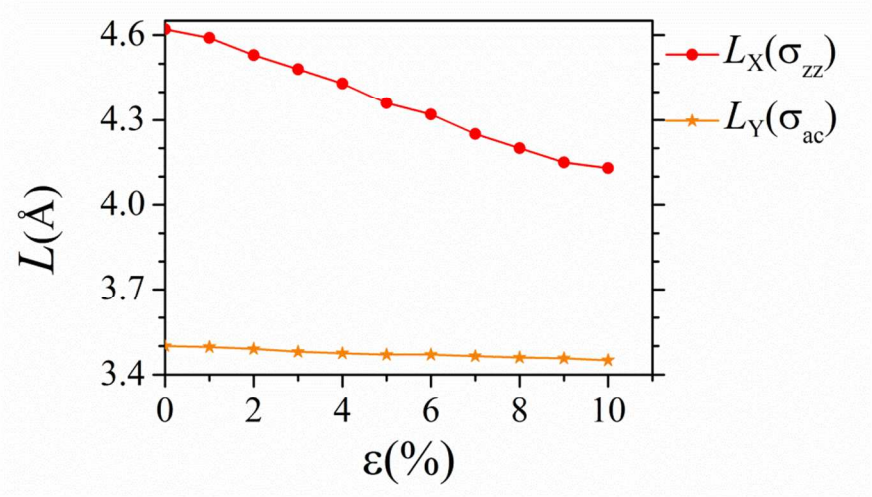

(b)

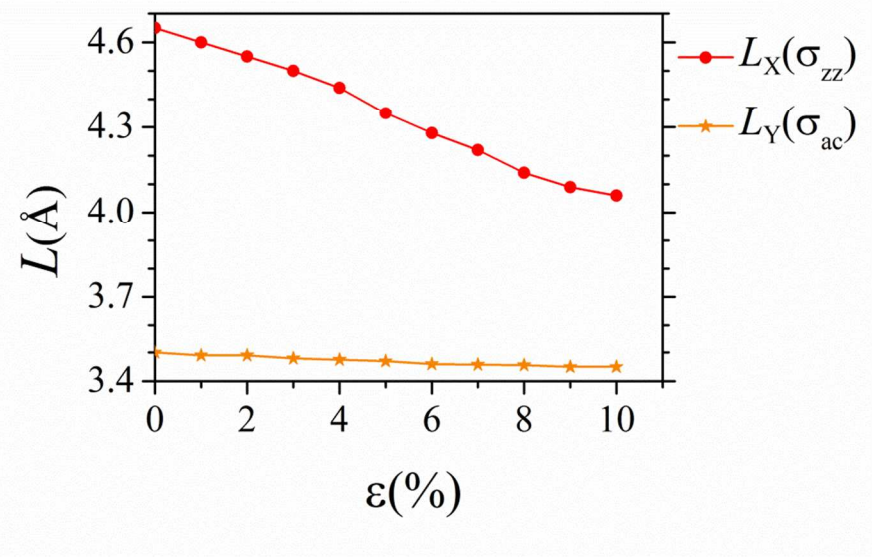

Figure S5 HSE06 band structures at 7 (a) and 10% (b) uniaxial strain along the armchair direction for the α_1 AsP.

(a)

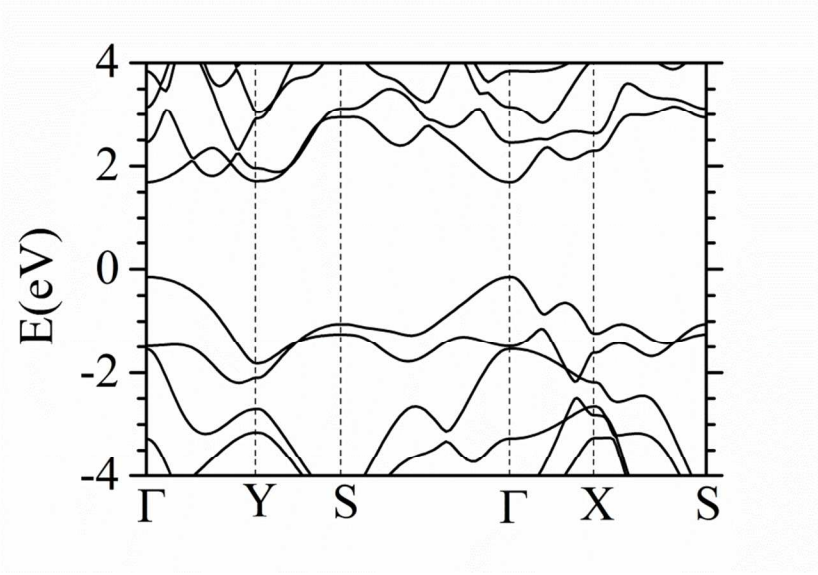

(b)

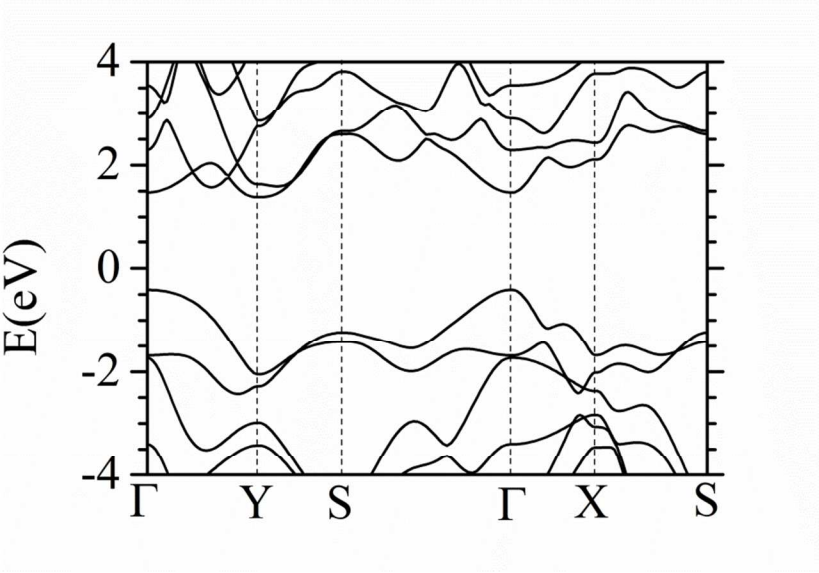

Figure S6 HSE06 band structures at 2 (a) and 7% (b) uniaxial strain along the zigzag direction for the α_1 AsP.

(a)

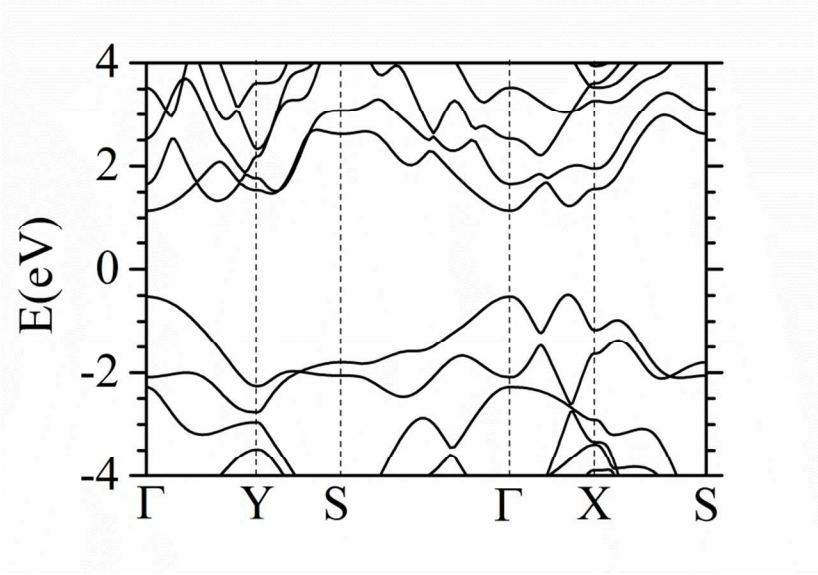

(b)